

## Computational Delay and Free Mode Environment Design for Haptic Display

Brian E. Miller<sup>1</sup> J. Edward Colgate<sup>1</sup> Randy A. Freeman<sup>2</sup>  
 Department of Mechanical Engineering<sup>1</sup>  
 Electrical and Computer Engineering<sup>2</sup>  
 Northwestern University  
 2145 Sheridan Rd  
 Evanston, IL 60208 USA

### Abstract

*This paper develops a technique for the design of haptic systems that guarantees the absence of oscillations. Valid components of the haptic system are general devices, virtual couplings and virtual environments, linear or nonlinear, however the current work focuses on linear components. Once developed, the method will be applied to a haptic system to investigate stability conditions for passive environments versus those for non-passive environments. Examples of computational delay and free mode environment design will be developed as meaningful design problems that fall into the category of non-passive environments.*

## 1 INTRODUCTION

A haptic display (or haptic device) is a mechanical device that lets users interact with computer generated environments. The haptic system considered in this work is a sampled-data system consisting of a haptic display, virtual coupling [6], and virtual environment. The concepts developed in this paper are applicable to general device models, virtual couplings and virtual environments which can take on both linear and nonlinear behavior. This paper will focus on linear components and in particular will investigate the interest in non-passive environments. Passivity tools will be used to identify a class of non-passive environments that can be displayed to the user in a passive manner.

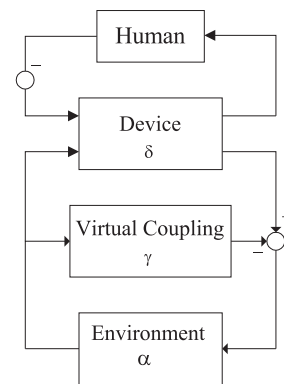


Figure 1: Graphical representation of the analysis.

Passivity has been a powerful tool in analyzing stability issues concerning dynamically coupled systems. Recently, it has been used to derive conditions for the passivity of the haptic display, as seen by the human operator. Previous work [3] [4] [1] [2] approached the problem by assuming that the human operator and virtual environment are passive, focusing on the haptic display and virtual coupling design.

Recently, work has been conducted placing more emphasis on the environment, and passivity has been used to investigate the range of environments that can be displayed passively. Previous work by the authors [10] presented a design methodology based on a parameterized concept (Figure 1) that guides design of the virtual coupling to ensure the absence of device driven oscillations, with the added benefit of being

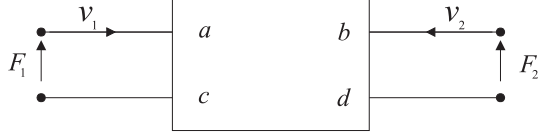


Figure 2: General two-port network.

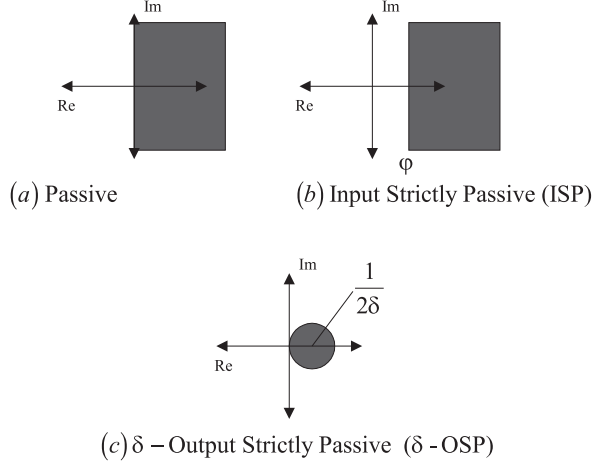


Figure 3: Levels of passivity.

able to identify the class of allowable virtual environments. This method was used to show that it is not necessary to assume that the environment is passive. Motivation for looking at nonlinear non-passive discrete-time environments was based on the fact that a significant class of passive continuous-time environments have non-passive discrete-time counterparts.

The goal of this paper is to consider linear non-passive environments to determine if they can be displayed passively, and moreover if they are of any practical interest in haptic display.

## 1.1 Stability Concepts

Two common techniques for analyzing the stability of two-port networks are passivity and unconditional stability. This section will introduce concepts associated with passivity in both the time domain and frequency domain.

The basic building block in two-port theory is shown in Figure (2). The force velocity pair  $(F_1, v_1)$  is measured at port a-c, and the pair  $(F_2, v_2)$  is measured at port b-d. The relationship between port parameters is provided by an immittance mapping between velocities  $(v_1, -v_2)$  and forces  $(F_1, F_2)$ . The minus sign on  $v_2$  comes about because when considering a

mapping from  $F_1$  to  $v_2$  it seems natural to consider a force  $F_1$  applied to the network to determine a velocity  $v_2$  leaving the network. To maintain that positive energy implies energy input to the network,  $v_2$  is defined positive flowing into the network. Possible immittance mappings include impedance (Z), admittance (Y), hybrid (H) and alternate hybrid (G). Work presented in [1] provides an elegant discussion on viewing haptic systems from traditional two-port network theory.

**Definition 1** A mapping from input ( $u$ ) to output ( $y$ ) is passive if and only if,

$$\int_0^t y(\tau)u(\tau)d\tau \geq 0, \forall t \geq 0 \quad (1)$$

Viewing the input and output signals as flow (velocity) and effort (force) variables Equation (1) states that the energy applied to a network must be positive for all time. The frequency domain interpretation is that the Nyquist plot lies in the closed right half plane (RHP), Figure (3).

**Definition 2** A mapping from input ( $u$ ) to output ( $y$ ) is output strictly passive (OSP) if and only if,

$$\int_0^t y(\tau)u(\tau)d\tau \geq \delta \int_0^t y^2(\tau)d\tau, \forall t \geq 0 \quad (2)$$

for some  $\delta > 0$ .

Output strict passivity (OSP) is a stronger level of passivity. Viewing the input and output signals as flow (velocity) and effort (force) variables Equation (2) states that the energy input to a network must be greater than or equal to the energy supplied by the network by a value  $\delta$  times the output squared. The frequency domain interpretation is that the Nyquist plot lies in a disk with radius  $\frac{1}{2\delta}$ , Figure (3).

**Definition 3** A mapping from input ( $u$ ) to output ( $y$ ) is input strictly passive (ISP) if and only if,

$$\int_0^t y(\tau)u(\tau)d\tau \geq \varphi \int_0^t u^2(\tau)d\tau, \forall t \geq 0 \quad (3)$$

for some  $\varphi > 0$ .

Input strict passivity (ISP) is a stronger level of passivity. Viewing the input and output signals as flow (velocity) and effort (force) variables Equation (3) states that the energy input to a network must be greater than or equal to the energy supplied by the network by a value  $\varphi$  times the input squared. The frequency domain interpretation is that the Nyquist plot lies to

the right of the vertical line at  $\varphi$  in the RHP, Figure (3). The discrete-time counterparts of the above definitions are defined by replacing the integral with a summation [7]. The Nyquist plots are the same.

To determine if a transfer function produces a passive mapping the following steps can be followed in order. If any of the conditions are violated the mapping is non-passive.

For a continuous-time transfer function  $E(s)$ :

- All poles must be in closed left half plane (LHP).
- Check for poles on  $j\omega$  axis:
  - Must be simple (single) poles.
  - Residue at the poles (located on  $j\omega$  axis) must be positive real.
- $Re\{E(j\omega)\} \geq 0 \forall \omega$  where  $E(j\omega)$  exists.

For a discrete-time transfer function  $E(z)$ :

- All poles must be in the closed unit disk.
- Check for poles on the unit circle:
  - Must be simple (single) poles.
  - Residues at the poles (located on the unit circle) must satisfy an angle condition: If a pole  $z_0$  exists on the unit circle then

$$\angle Res(E(z), z_0) = \angle z_0 \quad (4)$$

- $Re\{E(e^{j\theta})\} \geq 0 \forall \theta$  where  $E(e^{j\theta})$  exists

## 2 PROBLEM DEVELOPMENT

The goal of this work is to derive conditions under which the design of the haptic display guarantees the absence of oscillations under passive human excitation. The haptic display consists of a haptic device, virtual coupling and impedance virtual environment. The important characteristics (from a stability standpoint) of the haptic display and virtual coupling are represented by parameters  $\delta$  and  $\gamma$ , respectively. The next two sections will demonstrate how to compute these parameters. Restricting the scope to linear models will allow us to utilize  $\mu$ -synthesis tools.

The problem will be developed by first looking at the device model and placing an assumption on the level of passivity it must provide. Viewing the system in coupled stability form, a loop transformation [8] will be performed making it possible to analyze the system in two separate parts. The upper part consists

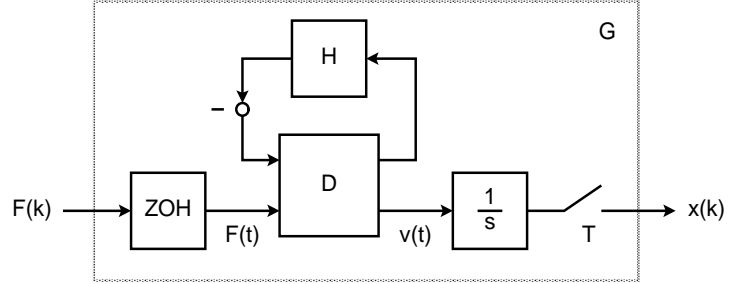


Figure 4: Device model: Zero-order hold equivalent.

of the device model and virtual coupling, and is required to be output strictly passive. The lower part includes the transformed environment, and is required to be passive. An output strictly passive block with a passive block in negative feedback remains output strictly passive. A nice duality exists for considering environments with admittance causality. Here, if the upper part is input strictly passive and the lower part passive a similar stability result exists. Finally, the discrete-time version of LaSalle's invariance principle [9] is invoked to guarantee the absence of oscillations.

## 3 Device Model

This section will introduce the device model along with the assumption on its behavior, Figure (4). The device model is discretized using the zero-order hold equivalent, which guarantees identical results with the continuous-time counterpart at each sample instant. This makes the stability results obtained for the discrete system valid for the original sampled-data system at the sample instants.

*Assumption:*  $\exists \delta > 0$  such that  $\forall$  passive  $H$ , mapping from  $F(t)$  to  $v(t)$  is  $\delta$ -OSP.

This assumption indicates that the device must possess sufficient damping to produce excess passivity in the system. It turns out that many devices in the literature satisfy this condition. Two methods exist to determine the value of  $\delta$ . An example will be given for a one degree of freedom haptic display.

For simple devices,  $\delta$  can be determined experimentally by injecting sine waves of varying frequency (constant amplitude). Force and velocity (computed from position) data can be recorded, and the Nyquist plot of the resulting transfer function can be plotted. To determine  $\delta$ , a disk is drawn such that it covers all the curves. The radius of this disk is equal to  $\frac{1}{2\delta}$ .

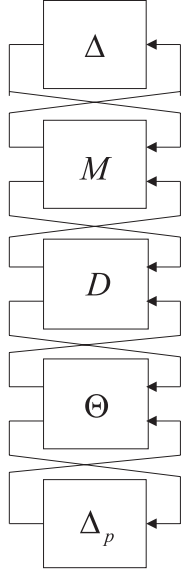


Figure 5: Robust stability problem

For a general two-port device model the parameter  $\delta$  can be determined by solving a robust stability problem. The robust stability problem is formulated using the above assumption about the OSP of the device along with augmented uncertainty ( $\Delta$ ). The next step is to transform the passivity conditions to small gain conditions. This development is similar to that presented in [5] with the important difference that the condition on the device is output strict passivity. Figure (5) reveals the structure of the problem. Blocks  $M$  and  $\Theta$  must be appropriately defined such that the passivity of the desired mapping is equivalent to a small-gain condition. Recall that the frequency domain condition for OSP is that the Nyquist plot lies in a disk of radius  $\frac{1}{2\delta}$ . Define  $J : F \rightarrow v$ , then if  $\|2J\delta - 1\|_\infty \leq 1$  the mapping  $J$  lies within the disk. This corresponds to

$$\Theta = \begin{bmatrix} 0 & 1 \\ 2\delta & -1 \end{bmatrix} \quad (5)$$

The augmented uncertainty comes from the assumption that the human behaves in a passive manner. Thus  $M$  must be defined such that  $\|\Delta\|_\infty \leq 1$ . Using the relationship,

$$H = \frac{1 - \Delta}{1 + \Delta} \quad (6)$$

the inter-connection between  $M$  and  $\Delta$  defines an upper linear fractional transformation (LFT) [11] pro-

ducing the following relationship:

$$M_{22} + M_{21}\Delta(1 - M_{11}\Delta)^{-1}M_{12} = \frac{1 - \Delta}{1 + \Delta} \quad (7)$$

The definition of  $M$  is not unique, however choosing  $M_{11} = -1$  the matrix is defined as follows:

$$M = \begin{bmatrix} -1 & 1 \\ 2 & -1 \end{bmatrix} \quad (8)$$

The generalized plant is computed using the star transform,  $G_p = M \star D \star \Theta$ , producing a diagonal two-block structured uncertainty problem. Conveniently, the two-block structured uncertainty problem produces an exact numerical result [11] giving us the value of  $\delta$ . The following example demonstrates this procedure on the one DOF haptic display from our lab.

*Example:* The model of the one DOF haptic display consists of a mass ( $m$ ) and damping ( $b$ ), represented in two-port form as follows:

$$D = \begin{bmatrix} \frac{1}{ms+b} & \frac{-1}{ms+b} \\ \frac{-1}{ms+b} & \frac{1}{ms+b} \end{bmatrix} \quad (9)$$

Computing the star transform

$$G_p = M \star D \star \Theta = \begin{bmatrix} G_{p11} & G_{p12} \\ G_{p21} & G_{p22} \end{bmatrix} \quad (10)$$

yields,

$$G_{p11} = \frac{-ms + (1 - b)}{ms + b + 1} \quad (11)$$

$$G_{p12} = \frac{-1}{ms + b + 1} \quad (12)$$

$$G_{p21} = \frac{-4\delta}{ms + b + 1} \quad (13)$$

$$G_{p22} = \frac{-ms + (2\delta - b - 1)}{ms + b + 1} \quad (14)$$

Since  $G_{12} \neq 0$  and  $G_{21} \neq 0$  we compute the scalar

$$\hat{d}_\omega = \sqrt{\frac{\|G_{p21}(j\omega)\|}{\|G_{p12}(j\omega)\|}} \quad (15)$$

Providing an initial guess for  $\delta$ , the largest singular value is computed at each frequency:

$$\mu_\Delta(G_p(j\omega)) \leq \bar{\sigma} \left( \begin{bmatrix} G_{p11}(j\omega) & \hat{d}_\omega G_{p12}(j\omega) \\ \frac{1}{\hat{d}_\omega} G_{p21}(j\omega) & G_{p22}(j\omega) \end{bmatrix} \right) \quad (16)$$

The largest value of  $\delta$  where  $\|\mu_\Delta\| \leq 1$  over the entire frequency range is the  $\delta$  for the device. For this example it turns out that  $\delta = b$ .

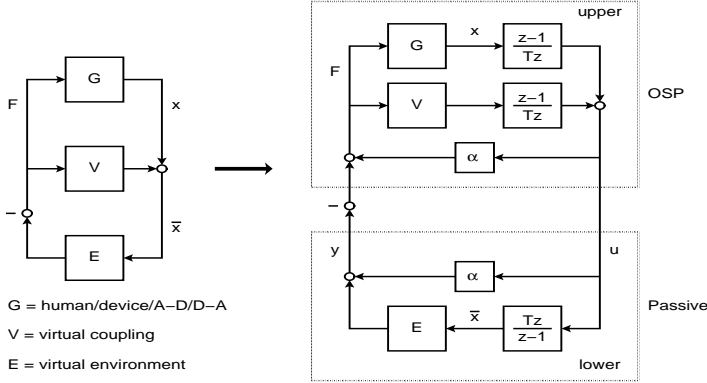


Figure 6: Loop Transformation.

## 4 Loop Transformation

Viewing the system in coupled stability form, Figure (6), a loop transformation is performed [8] to obtain an equivalent but expanded view of the haptic system. The expanded view of the system consists of an upper part that must be OSP and a lower part that must be passive. A mapping between velocity and force is needed for a passivity analysis, therefore a multiplier is added in the appropriate locations (a velocity measure is not assumed since position is read via encoder in practice). The parameter  $\alpha$  represents the amount of excess passivity (in the form of damping) available to the environment. The expanded view of the haptic system reveals an important relationship:  $\alpha$  is in positive feedback with the parallel combination of the device and virtual coupling producing a destabilizing effect. Viewing the excess damping in the lower part of the system it turns up in feedforward with the environment, providing a stabilizing effect. This says that the environment can exhibit non-passive behavior by an amount related to  $\alpha$ . Therefore, increased damping in the device allows for a larger degree of non-passive behavior in the environment. The trade-off is that the inherent damping continues to increase in conflict with device transparency concerns. Viewing the system in this form allows us to analyze the upper and lower parts separately.

### 4.1 Upper Subsystem

The condition imposed on the upper part is that it must be OSP. The analysis is difficult because this part includes the class of passive human operators. This means that passivity conditions would need to be checked on an infinite number of mappings.

To eliminate this difficulty the following approach

is taken. Given that  $\delta > 0$  and

$$\alpha < \delta \quad (17)$$

$$\gamma > \frac{\delta\alpha}{\delta - \alpha} \quad (18)$$

we define:

$$Q = \frac{(z-1)}{Tz} \left[ V - \frac{T}{2\delta} \right] \quad (19)$$

If  $Q$  is  $\gamma$ -OSP then the upper part is OSP. The proof is omitted to conserve space, however the expression  $Q$  provides a relationship between the device and virtual coupling design.

### 4.2 Lower Subsystem

In this section we consider discrete-time passive linear shift-invariant (LSI) environments as well as non-passive LSI environments. The relationship between the environment and  $\alpha$  will be investigated for both. Although the results presented in this paper are valid for linear or nonlinear components, since we are restricting ourselves to the linear domain we will use the frequency domain interpretation.

#### 4.2.1 Passive Linear Environments

The first step in analyzing the lower part is to determine if the environment mapping from velocity to force is passive. The steps laid out in Section 1.1 are used. For passive environments,  $\alpha \equiv 0$  and the assumption on the lower part is satisfied. The parameter  $\alpha$  is set to zero for passive environments since a non-zero  $\alpha$  only serves to destabilize the upper subsystem.

Now consider a  $-K$  inserted in the environment block. The exclusion of negative environments can be observed by checking the residue of  $\frac{y}{v} = -K \frac{Tz}{z-1}$  and verifying that it violates the residue condition of Equation (4). For this particular transfer function the residue is negative implying that the arc encloses the entire LHP, therefore an infinite  $\alpha$ , corresponding to a device with infinite damping, would be needed to shift the Nyquist plot back into the RHP. Obviously this is an unrealistic situation in practice.

#### 4.2.2 Non-passive Linear Environments

Non-passive linear environments can be identified in the frequency domain as having some part of the Nyquist curve in the LHP. Using the steps in Section 1.1 a non-passive environment will violate one of

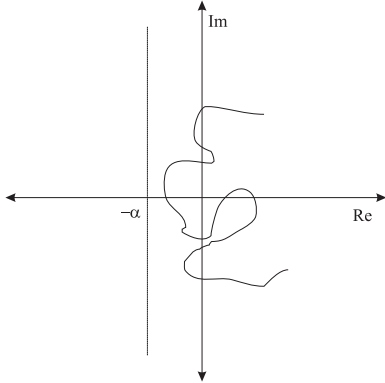


Figure 7: Valid location of the Nyquist region for  $\frac{Tz}{z-1}E(z)$ .

the conditions. After checking that the poles are contained in the closed unit disk the residue condition can be checked for any simple poles on the unit circle. Then we focus on  $Re\{\frac{T e^{j\omega T}}{(e^{j\omega T}-1)}E(e^{j\omega T})\}$  to see if an  $\alpha < \delta$  exists to shift the curve back into the RHP. This can be seen graphically in Figure (7).

The ability to shift the Nyquist plot back into the RHP depends on device parameter  $\delta$ , since the condition  $\alpha < \delta$  must hold. Therefore, some non-passive environments will only be valid if device parameter  $\delta$  is increased. For the high bandwidth force display [2], a  $\mu$ -calculation was performed that determined  $\delta = b_4$ . To increase the class of non-passive environments that can be displayed passively, damper  $b_4$  would need to be increased.

## 5 DESIGN RESULTS

Recall the important design variables identified throughout the development.

- $\delta$  represents an OSP condition on the device and can be obtained through experimental means, or by formulating a robust stability problem and performing a  $\mu$ -computation.
- $\gamma$  represents an OSP condition on the virtual coupling. The  $\gamma$ -OSP condition must be satisfied by  $Q$ . The implication of this construction is that for a  $\delta$ -OSP device model and  $\gamma$ -OSP  $Q$ , the upper part is OSP for every passive  $H$ .

Recall the design inequalities that must hold:

- $\alpha < \delta$
- $\gamma > \frac{\delta\alpha}{\delta-\alpha}$

A special case is encountered when the virtual coupling is a pure stiffness equal to  $\frac{2\delta}{T}$ . For this situation  $Q = 0$  and condition (18) automatically holds.

Suppose we have a haptic device and would like to determine the class of environments that can be displayed passively. We would begin the design by determining the damping parameter  $\delta$  either experimentally or through a  $\mu$ -computation. Then we can choose  $0 \leq \alpha < \delta$ . The class of environments that can be displayed passively have Nyquist plots that lie to the right of the vertical  $-\alpha$  line, Figure (7).

Consider a task where the class of environments is well characterized. Drawing the Nyquist plot of these environments the minimum value of  $\delta$  can be found by bounding the environment curves from the left. Once the device has been assembled the virtual coupling can be designed. The design of the virtual coupling is closely related to the amount of damping ( $\delta$ ) in the device. Assuming a virtual coupling with pure stiffness, there exists a design inequality where  $\gamma = \frac{\delta KT}{2\delta - KT} > 0$ . This is achieved if  $\delta > \frac{KT}{2}$ . Therefore, as the damping characteristic  $\delta$  is reduced either the virtual coupling stiffness must be reduced or the sampling rate must be increased. Finally, if a device exists and a desired class of environments is known then the desired results can be obtained by adjusting the sample period ( $T$ ).

## 6 MOTIVATING EXAMPLES

This section will investigate two motivating examples that require non-passive linear environments: delayed springs and free mode environment design. The next section will consider a delayed implementation of the virtual wall. Computational delay is often a necessary step during implementation. The ability to incorporate it into the stability analysis brings the theoretical development closer to actual implementation.

An important part in haptic display applications is free mode, where it is desired to make the haptic device transparent to the user. Since a certain class of non-passive environments are allowed, it may be possible to simulate free mode through environment design without changing virtual coupling parameters.

Figure (8) shows the transformed environment where the mapping from  $u$  to  $y$  must be passive. Assuming the existence of a haptic device with  $\delta > 0$  (a function of device damping), an  $\alpha < \delta$  can be found that shifts the Nyquist plot into the closed RHP. Therefore, a valid Nyquist plot for the environment  $E$  is one that lies to the right of the vertical line  $-\alpha$ .

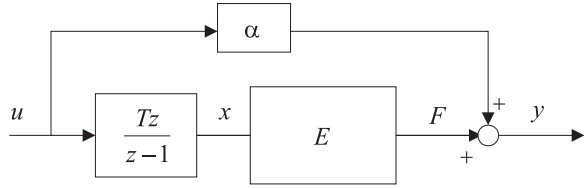


Figure 8: Environment block with parameter  $\alpha$ . The mapping from  $u$  to  $y$  must be passive.

## 6.1 Delayed Spring

Consider the example of a simple delayed spring,  $E(z) = \frac{K_E}{z}$ . The result is that a limit is placed on the amount of environment stiffness that can be programmed. We proceed by computing the transfer function  $S(z)$  between output  $y$  and input  $u$

$$S(z) = \frac{K_E T}{z-1} + \alpha \quad (20)$$

The task is to determine under what condition the mapping from  $u$  to  $y$  in Figure (8) is passive. The steps listed in Section 1.1 will be used. Because of the delay in the environment, a passive mapping will never exist in the bottom path that goes only through the integrator and environment ( $E$ ). However, recall that  $\alpha$  is a damping parameter and therefore has a direct effect on the real part of the transfer function. After verifying that the residue condition is satisfied, we can focus on  $Re\{S(e^{j\omega T})\}$ . The class of delayed springs that can be displayed passively is

$$\alpha = \frac{1}{2}K_E T < \delta \quad (21)$$

## 6.2 Free Mode Operation

Another motivation for non-passive linear environments is free mode operation without changing virtual coupling parameters. For example, consider the goal of eliminating the effect of physical damping in the device. We begin by viewing the haptic system completely in continuous-time to determine the necessary environment to cancel the influence of physical damping. The problem will be formulated in the following way:

- Determine the continuous-time version of the environment that cancels the physical damping ( $b$ ) so that  $\frac{1}{ms+\epsilon}$  is perceived by the operator. The parameter  $\epsilon \geq 0$  can be used to tweak the environment to satisfy stability conditions at the expense of some damping felt by the operator.

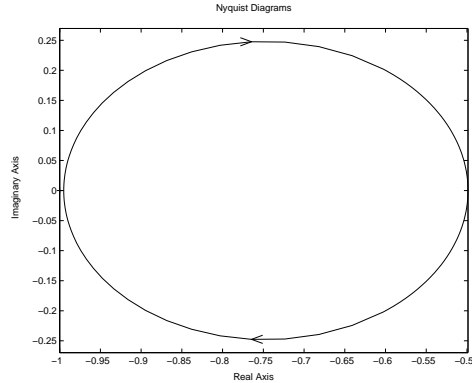


Figure 9: Nyquist plot of  $\frac{Tz}{z-1}E(z)$

- Obtain a discrete-time approximation of this environment.
- Verify that it meets the necessary criteria to help guarantee the absence of oscillations.

For this example we will assume a virtual coupling of pure stiffness equal to  $\frac{2b}{T}$  ( $\delta = b$ ). The continuous-time environment that results in a combined device, virtual coupling and environment block (Figure 1) of  $\frac{1}{ms+\epsilon}$  is

$$E(s) = \frac{2b(b-\epsilon)s}{T(\epsilon-b)s-2b} \quad (22)$$

Obtaining a discrete-time version using the backward difference approximation

$$E(z) = \frac{2b(b-\epsilon)z + 2b(\epsilon-b)}{(T\epsilon-3Tb)z + (Tb-T\epsilon)} \quad (23)$$

It can be shown that the environment/virtual coupling feedback loop is well-posed if  $T \neq \frac{1}{3}$ .

To determine if this satisfies our conditions, we place the environment in the block diagram of Figure (8). The parameter  $\alpha$  has units of damping and for  $\alpha > 0$  will shift the entire Nyquist plot to the right.

Following the steps in Section 1.1, we can determine if an  $\alpha$  exists such that the mapping from  $u$  to  $y$  in Figure (8) is passive. The only pole is located at  $z = \frac{(b-\epsilon)}{(\epsilon-3b)}$ . In the limit as  $\epsilon$  approach zero, the pole approaches  $\frac{1}{3}$ . No poles exist on the unit circle so the residue condition does not need to be checked. The final condition is that  $Re\{\frac{T e^{j\omega T}}{e^{j\omega T}-1}E(e^{j\omega T}) + \alpha\} \geq 0$ . Since at this point we are looking for an  $\alpha$  a more constructive way to view this is that we need  $Re\{\frac{T e^{j\omega T}}{e^{j\omega T}-1}E(e^{j\omega T})\} \geq -\alpha$  where ( $\alpha < b$ ). Taking

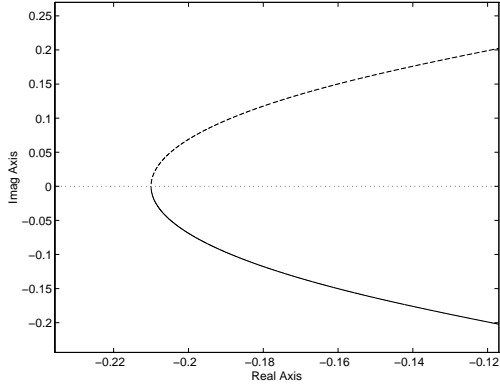


Figure 10: Nyquist region associated with a delay spring/damper virtual wall. The critical point is at  $-b = -0.22$ .

$b = 1$ ,  $T = .001$  and  $\epsilon = .005$  the Nyquist plot of  $\frac{Tz}{z-1}E(z)$  is shown in Figure (9). We see that the Nyquist plot falls to the right the critical  $-b = -1$  point, therefore an  $\alpha < \delta$  exists to shift the entire curve back into the RHP. Increasing  $\epsilon$  will allow us to meet the condition more strictly, however at the expense of some damping felt by the operator.

The next section will consider a bench mark example in the field of haptics to demonstrate the effect of computational delay.

## 7 DELAYED VIRTUAL WALL

This section will investigate a delayed version of a backward difference spring/damper virtual wall.

$$E(z) = \frac{(K_E T + B_E)z - B_E}{Tz^2} \quad (24)$$

The one DOF haptic display exhibits approximately  $b = .22 \frac{Nm-sec}{rad}$  of physical damping. Stiffness and damping parameters as designated

$$K_E = 220 \frac{Nm}{rad} \quad (25)$$

$$B_E = .1 \frac{Nm-sec}{rad} \quad (26)$$

Next we compute the Nyquist plot of

$$\frac{Tz}{z-1}E(z) = \frac{(KT + B)z - B}{z(z-1)} \quad (27)$$

From the Nyquist plot it is clear that an  $\alpha < \delta$  ( $\delta = b$ ) exists to shift the Nyquist plot such that it lies in the closed right half.

It is important to note that the environment stiffness is half of the virtual coupling stiffness. Increasing either the environment stiffness or damping will cause the Nyquist curve to cross the  $-\alpha$  line, thus violating our condition.

## 8 SUMMARY AND CONCLUSION

This paper developed a technique for the design of haptic systems that guarantees the absence of oscillations. A certain class of non-passive linear environments can be displayed in a passive manner to the user, and examples were provided to show that this class includes environments of interest. The results of this paper were developed using frequency domain concepts because the scope was restricted to linear systems. These results extend to nonlinear components where the results are presented in the time domain.

## References

- [1] R. Adams and B. Hannaford, "A Two-Port Framework for the Design of Unconditionally Stable Haptic Interfaces," *Proc. IEEE/RSJ International Conference on Intelligent Robots and Systems*, 1998.
- [2] R. Adams and B. Hannaford, "Stability Performance of Haptic Displays: Theory and Experiments," *Proc. International Mechanical Engineering Congress and Exhibition*, ASME, Anaheim, CA, Vol.SAX-64,p.227-234, 1998.
- [3] J.M. Brown and J.E. Colgate, "Minimum Mass for Haptic Display simulations," *Proc. International Mechanical Engineering Congress and Exhibition*, ASME, Anaheim, CA, Vol.SAX-64, p.249-256, 1998.
- [4] J.M. Brown and J.E. Colgate, "Passive Implementation of Multibody Simulations for Haptic Display," *Proc. International Mechanical Engineering Congress and Exhibition*, ASME, Dallas, TX, Vol.DSC-61, p.85-92, 1997.
- [5] J.E. Colgate and G.G. Schenkel, "Passivity of a class of sampled-Data systems: Application to Haptic Interfaces," *Journal of Robotic Systems*, Vol. 14(1), p.37-47, 1997.
- [6] J.E. Colgate, M.C. Stanley and J.M. Brown, "Issues in the Haptic Display of Tool Use," *Proc. IEEE/RSJ International Conference on Intelligent Robots and Systems*,1995.
- [7] G.C. Goodwin and K.S. Sin, *Adaptive Filtering Prediction and Control*, Englewood Cliffs, 1984.
- [8] H. Khalil, *Nonlinear Systems*, Prentice-Hall Inc., 1996.
- [9] J.P. LaSalle, *Stability and Control of discrete Processes*, Springer-Verlag, New York, 1986.
- [10] B.E. Miller, J.E. Colgate and R.A. Freeman, "Passive Implementation for a Class of static Nonlinear Environments in Haptic Display," *IEEE International Conference on Robotics and Automation*, 1999.
- [11] K. Zhou and J. Doyle, *Essentials of Robust Control*, New Jersey, 1965.